Received: 2 August 2020 | Revised: 4 February 2021 | Accepted: 21 February 2021

DOI: 10.1002/jcc.26512

FULL PAPER

Journal of COMPUTATIONAL CHEMISTRY WILEY

Drug repositioning to target NSP15 protein on SARS-CoV-2 as possible COVID-19 treatment

Yudibeth Sixto-López Ph. D. | Marlet Martínez-Archundia

Laboratorio de Diseño y Desarrollo de Nuevos Fármacos e Innovación Biotecnológica (Laboratory for the Design and Development of New Drugs and Biotechnological Innovation), Sección de Estudios de Posgrado e Investigación
Escuela Superior de Medicina, Instituto Politécnico Nacional, Plan de San Luis y Salvador Díaz Mirón s/n, Casco de Santo Tomás, Ciudad de México, Mexico

Correspondence
Marlet Martínez-Archundia Laboratorio de Diseño y Desarrollo de Nuevos Fármacos e Innovación Biotecnológica (Laboratory for the Design and Development of New Drugs and Biotechnological Innovation), Sección de Estudios de Posgrado e Investigación Escuela Superior de Medicina, Instituto Politécnico Nacional, Plan de San Luis y Salvador Díaz Mirón s/n, Casco de Santo Tomás Ciudad de México 11340, Mexico,
Email: marletm8@gmail.com; mtmartineza@ipn.mx

Funding information
Instituto Politécnico Nacional

Abstract

SARS-CoV and SARS-CoV-2 belong to the subfamily Coronaviridae and infect humans, they are constituted by four structural proteins: Spike glycoprotein (S), membrane (M), envelope (E) and nucleocapsid (N), and nonstructural proteins, such as Nsp15 protein which is exclusively present on nidoviruses and is absent in other RNA viruses, making it an ideal target in the field of drug design. A virtual screening strategy to search for potential drugs was proposed, using molecular docking to explore a library of approved drugs available in the DrugBank database in order to identify possible NSP15 inhibitors to treat Covid19 disease. We found from the docking analysis that the antiviral drugs: Paritaprevir and Elbasvir, currently both approved for hepatitis C treatment which showed some of the lowest free binding energy values were considered as repositioning drugs to combat SARS-CoV-2. Furthermore, molecular dynamics simulations of the Apo and Holo-Nsp15 systems were performed in order to get insights about the stability of these protein-ligand complexes.

KEYWORDS
COVID-19, Elbasvir, molecular dynamic simulation, Nsp15, Paritaprevir, SARS-CoV-2

1 | INTRODUCTION

Coronaviruses (CoV) belong to the subfamily *Coronaviridae* and they are enveloped and single positive-stranded RNA viruses.[1] These viruses are distinctive for showing spike projections which stand from the virion surface resembling a crown. The coronavirus SARS-CoV causes the SARS disease, which first appeared in late 2003 in China, and since then, it was clear that a swift and reliable diagnosis was needed. SARS-CoV shows a positive strand RNA genome of about 30 kb in length.[2] By the end of 2019, a new type of coronavirus was identified in Wuhan, a Chinese province. Sometime later, this virus was identified as SARS-CoV-2 by the International Committee on Taxonomy of Viruses (ICTV).

SARS-CoV-2 belongs to lineage B β-CoVs, subgenus *Sarbecovirus*.[3] Structurally, SARS-CoV and SARS-CoV-2, are formed by four main proteins: Spike glycoprotein (S), membrane (M), envelope (E), and nucleocapsid (N).[1] Particularly, the S protein mediates the binding of the receptor to the Host through receptor binding domains (RBD).[1,4] The genome of SARS-CoV-2 and also codifies for non-structural proteins (Nsps) contained in a replicase gene that, due to ribosomal frameshifting, it encodes for two ORFs: rep1a and rep1b. These are then translated into two polyproteins named: Pp1a and Pp1ab, which are processed into 3C-like proteases, encoded by Nsp5 (3CLpro), as well as a papain-like protease encoded by Nsp3 (PLP). After being processed, it yields into 16 viral Nsps, one of which is the Non-structural protein 15 (Nsp15). Nsp15 encodes a nidoviral RNA uridylate-specific endoribonuclease (NendoU), that is highly conserved among vertebrate nidoviruses (coronaviruses and arteriviruses). It plays a critical role in the viral replication and transcription.[5,6] Nsps in other coronaviruses, assemble into a membrane-associated replicase-transcriptase complex, with many other functions that are yet to be elucidated.[7]

SARS-CoV and SARS-CoV-2 are two (out of seven) beta coronaviruses that are able to infect humans. These two CoV share a higher sequence identity in their constitutive proteins, such as the subunit 2 of the S protein (89.8%),[8] as well as the Nsp15 protein (88% sequence identity and 95% similarity). Structurally, they are also very

similar, showing RMSD values of 0.47 Å (SARS-COV chain A; PDB id: 2H85 and SARS-CoV-2 chain A; PDB: 6VWW).[6]

Particularly, the SARS-CoV Nsp15 protein, produced in *Escherichia coli*, has endoribonuclease (endoU) activity that preferentially cleaved the 5′ of uridylates of RNAs.[9] Similar EndoU activities have been described in other CoV Nsp15s, including human CoV 229E, mouse hepatitis virus (MHV), avian infectious bronchitis virus (IBV), turkey CoV (TcoV).[10,11] Some years ago, it also was proposed that the EndoU activity of Nsp15, could interfere with the innate immune response.[11,12]

The Nsp15 proteins from SARS-COV and SARS-COV-s are structurally very similar. Nsp15 is an hexameric endoribonuclease with a catalytic site formed by two Histidine residues and a Lysine residue, which is a similar characteristic to RNase A.[6,7] Nsp15 forms a hexamer made of dimers of trimers. The 39 kDa monomeric unit, composed of ~345 residues, folds into three domains: N-terminal, middle domain, and the C-terminal catalytic NendoU domain, which is the domain responsible for the catalytic activity. Additionally, Nsp15 is exclusively present on nidoviruses and is absent in other RNA viruses, making it as an ideal target for drug design, to combat SARS-CoV-2.[13,14] Therefore, in this work, we aim to identify Nsp15 inhibitors with a virtual screening strategy through molecular docking analysis and by employing some of the approved drugs from the library of DrugBank database. Then, we performed molecular dynamics simulations, in order to study the stability and structural properties of the apo-Nsp15 as well as the ligand-Nsp15 complexes, which could provide insights about their potential use in the treatment for the Covid-19 disease.

2 | METHODS

2.1 | Ligands

In total, we retrieved 2467 ligands from the Drugbank database (https://www.drugbank.ca/), specifically considering only the approved for human. The ligands were further processed using Raccon,[15] a graphical user interface for AutoDock virtual screening, in order to transform them to a suitable format (pdbqt), for further molecular docking studies. In this procedure, only polar hydrogens were taken into account and Gasteiger charges were also added.

2.2 | Molecular docking

Focused molecular docking studies were carried out using Autodock vina.[16] Nsp15 protein structure of SARS-CoV-2 (PDB: 6VWW) and the Nsp15 protein for the SARS-CoV (PDB: 5H85) were retrieved from Protein Data Bank (PDB).

In total, 2467 ligands were tested against Nsp15. The grid box of was centered on catalytic residues: H235, H250, K290, T341, Y343, and S294 with grid box dimensions of 30 Å × 30 Å × 30 Å.[6] Compounds were prepared using Racoon,[15] while protein was prepared with AutoDock Tools 1.6.5.[17] Polar hydrogen atoms and Kollman charges were encompassed. The molecular docking process was carried out using Autodock Vina.[16] Virtual screening was carried out only on SARS-CoV-2 Nsp15, from which only the compounds with the lowest free energy of binding were retrieved. Then, those compounds were also tested against SARS-COV Nsp15, under the same molecular docking conditions stated above. Benzopurpurin B, the experimental SARS-CoV in vitro Nsp15 inhibitor, was employed as a positive control. Additionally, we could observe that our molecular docking approach reproduced the interactions previously reported, validating our docking procedure.

2.3 | Molecular dynamic simulation

Molecular dynamic simulations of the apo (Nsp15) and holo (Nsp15-Elbasvir and Nsp15-Paritaprevir and Nsp15-Citrate), were carried out using the GROMACS package. This procedure was done by employing the OPLS force field for GROMOS (GROMACS 96).[18] The box dimension was settled at least 1.0 nm away from the wall of the dodecahedral box with periodic boundary conditions, solvated with SPC water molecules. Systems were neutralized with 12 atoms of Na. Energy minimization was carried out using the steepest descent method. Berendsen temperature coupling and isotropic pressure coupling were established in order to reach a stable environment (300 K, 1 bar). The particle mesh Ewald (PME) algorithm was applied to treat electrostatic and Van der Waals interactions, using the following values: cutoff for the short-range VdW (rvdw) was set to 1.0 nm and Coulomb cut-off (r coulomb) at 1.0 nm. All the bond lengths were constrained using the LINCS algorithm[19] and the time step was set to 0.002 ps. The complex was equilibrated for 10 ns, and the MD simulations were run for about 30 ns. MD simulations were further processed, by the removal of translational and rotational movements from the systems, before the calculation of the root-mean-square deviation (RMSD) and root-mean-square fluctuations (RMSF).

Conformational sampling of the protein was considered at 0, 10, 20, and 30 ns. Additionally, representative ensembles were obtained by RMSD conformational clustering algorithm using the GROMOS method.[20]

We then performed a principal component analysis (PCA), also known as essential dynamic (ED). The PCA analysis is a statistical technique that allows to extract the large-scale collective motions of the atoms from the simulations, that are often correlated to its biological function and biophysical properties.[21] The performed method is described in detail elsewhere.[22] Citrate molecule was included in the MD simulation studied; due to the fact, it was reported to be bound to the Nsp15 catalytic site of SARS-CoV-2.[6]

3 | RESULTS AND DISCUSSION

3.1 | Virtual screening

A virtual screening strategy, by means of Autodock Vina was carried out while employing only the approved compounds for human use,

retrieved from the Drugbank database. A total of 2467 ligands were docked against Nsp15 SARS-CoV-2, from which 16 ligands were selected due to their lowest free binding energy, that spans from −10.9 to −9.0 kcal/mol (Table 1).

These drugs are currently approved by the market with different indications. Difenoxine and Levocanbastine depicted free binding energy values lesser than −10.5 kcal/mol. However, Difenoxine is a controlled drug since it belongs to the opioids agents, while Levocabastine is for ophthalmic use. Other types of compounds that showed good free binding energy were Digoxin, Deslanoside, Acetyldigitoxin. Digitoxins are cardiac glycosides that show a sterol group as part of their chemical scaffold (Table 1). In early 2020, Ciclesonide, an inhaled steroid, was suggested to target Nsp15 by in vitro studies, specifically for coronavirus.[23] Thus, our findings might explain that the presence of sterol moiety, can be considered as a scaffold to target NSP15, and this group is needed and constitutes the first approach for further chemical modifications, with the aim to achieve better selectivity as well as the improvement of their ADMET properties. The use of Deslanoside, Digitoxin, and Acetylditgitorin, which are glycoside cardiotonics were not contemplated for further studies, since they usually have a narrow therapeutic margin, hindering the administration or patient adherence.

Ivosidenib, Entrectinib, and Irinotecan are drugs approved for cancer treatments, like leukemia, non-small cancer cell lung, and colorectal cancer, respectively, however, due to their several side effects, they were not considered for this study. In the case of sibutramine, this drug also depicted a good free binding energy (−9.8 kcal/mol) but it was recently withdrawn due to safety effects (cardiovascular events and strokes), and it was the reason it was not considered neither in this study. Atovaquone and Bedaquiline (−9.7 and − 9.6 kcal/mol, respectively) showed also favorable free binding energies, and they are used as antimalarial and antimycobacterial drugs, respectively. Atovaquone was also used in an independent study as Mpro ligand for SARS-CoV-2 treatment. Thus, our approach proposes Atovaquone

TABLE 1 Affinities of the compounds for Nsp15 protein of SARS-CoV-2 and SARS-COV obtained by virtual screening using Autodock Vina

Free energy of binding (kcal/Mol)				
SARS-CoV-2	**SARS-COV**	**Name**	**Drugbank ID**	**Indications**
−10.9	−9.8	Difenoxina	DB01501	It acts as a potent antidiarrheal by slowing the movement of the intestines. It is an opioid agent.
−10.6	−9.8	Levocabastine	DB01106	H1-receptor antagonist used for allergic conjunctivitis.
−10.3	−9.4	Digoxin	DB00390	Digoxin is classified as a cardiac glycoside used to manage atrial fibrillation.
−10.2	−9.7	Ivosidenib	DB14568	Isocitrate dehydrogenase-1 (IDH1) inhibitor approved for use in acute myeloid leukemia.
−10.1	−9.5	Deslanoside	DB01078	Cardiotonic glycoside for the treatment and management of Congestive cardiac insufficiency, arrhythmias and heart failure.
−10	−9.3	Dihydroergotamine	DB00320	For the acute treatment of migraine headaches with or without aura and the acute treatment of cluster headache episodes.
−10	−8.8	Acetyldigitoxin	DB00511	Cardioactive derivative of lanatoside A or of digitoxin used for fast digitalization in congestive heart failure.
−9.8	−4.8	Sibutramina	DB01105	For the treatment of obesity.
−9.7	−9	Atovaquone	DB01117	It has antimicrobial and antipneumocystis activity. It is being used in antimalarial protocols.
−9.7	−8	Entrectinib	DB11986	It is indicated for the treatment of metastatic ROS1-positive non-small cell lung cancer in adults.
−9.6	−9	Ergotamine	DB00696	It is a vasoconstrictor to treat migraine disorders.
−9.6	−9.7	Digitoxin	DB01396	It is a cardiac glycoside sometimes used in place of digoxin.
−9.6	−8.9	Bedaquiline	DB08903	Bactericidal antimycobacterial drug to treat pulmonary muli-drug resistant tuberculosis (MDR-TB).
−9.6	−11.1	Paritaprevir	DB09297	It is indicated for the treatment of chronic hepatitis C virus.
−9.6	−8.7	Elbasvir	DB11574	Antiviral medication used as part of combination therapy to treat chronic hepatitis C; an infectious liver disease caused by infection with hepatitis C virus.
−9.5	−8.5	Irinotecan	DB00762	It is an antineoplastic enzyme inhibitor primarily used in the treatment of colorectal cancer.
−9.0	−8.7	Benzopurpurin_b		In vitro inhibitor of Nsp15[7]

for COVID-19 treatment, due to its possible binding to Nsp15.[24] Additionally, Ergot derivatives, such as Dihydroergotamine and Ergotamine (−10 and − 9.6 kcal/mol, respectively) were also pointed out as possible ligands that target Nsp15, since they both are used for migraine treatment. Independently, ergotamine was proposed as a Mpro ligand, identified by combining molecular docking and MD simulation studies,[25] and it also was proposed to target several SARS-CoV-2 proteins such as: Nsp1, 2, 4, 5, 7, 8, 9, 10, and 12, papain-like proteinase, proteinase 3CL-PRO, RdRp, spike protein, Mpro, and others, making it a potential drug to be used for COVID-19 treatment.[25] Finally, Paritaprevir and Elbasvir, two antiviral drugs currently approved for hepatitis C treatment, depicted a binding free energy of −9.6 kcal/mol each. Thus, they were considered for further MD simulation studies, aside from the fact that independent studies have suggested the use of both compounds for COVID-19 treatment.[24,25] (Scheme 1).

3.2 | Molecular docking

From the molecular docking studies, we could observe that the 15 compounds showed similar binding modes, due to their common chemical moieties, as discussed below.

Difenoxin and levocabastine complexes with Nsp15-SARS-CoV-2 show mainly hydrophobic interactions, by making π-π interactions with phenyl rings of residues H235 and Y343, and also showing π-cation interactions with K290; while on the other extreme, the phenyl groups interact with W333 through π-π interactions. Thus, the aromatic interactions seem to be crucial for both compounds, which are complemented with hydrogen bonding interactions at G248, H250, H235, and K290, with carboxylic group of both molecules (Figures 1A and 2E,N).

Deslanoside, Acetyldigitoxin, Digitoxin, on the other hand, share a similar binding mode, since they accommodated their glycoside portion into the catalytic site, by interacting through π-π or hydrophobic interactions with W333, Y343, K290, as well as hydrogen bonds with H235, H250, T341, S294, V292. The sterol portion mainly interacts with M219 and F241 (Figures 1B and 2A,F,D).

Digoxin, as the other molecules, accommodates the glycoside portion into the catalytic site but the sterol portion interacts with different residues, in comparison to other ligands: Deslanoside, Acetyldigitoxin, and Digitoxin. Docking studies suggested that Digoxin interacts with H235 and V339, by hydrophobic interactions, and forming hydrogen bonds with G230, E340, A232, and E234 (Figure 2G). Therefore, for this group of molecules, it seems that the glycoside portion might play a preponderant role in the recognition of the Nsp15 catalytic site. Parallel to this work, another research group found that, Digitoxin and Digoxin, displayed a moderate anti-SARS-CoV-2 and anti-MERS-CoV activity. Such activity could be due to the Nsp15 inhibitory effect. Thus, this could be related to the fact that the SARS-CoV-2 shows high similarity.[27,28]

Entrectinib accommodates the benzimidazole and the difluoro-substituted phenyl ring along the catalytic site, in which the benzimidazole moiety interacted with Y343 via π-π, with H346, K345, and H250 via hydrophobic interactions, and with H235 and S240 via hydrogen bonds (Figures 1E and 2K). In the case of Ivosidenib, its binding mode resembles that of Entrectinib, by accommodating the aromatic rings aside of the catalytic cleft, and interacting with important residues such as H250, T341, and Y343. Here, the disubstituted cyclobutene moiety interacts with E245 and C291 (Figures 1E and 2L). Both compounds were able to form hydrogen bonds, π-π interactions, and halogen interactions, features that can further be taken into account for potential drug design strategies.

Both Bedaquiline and Atavaquone, in both cases accommodate the quinoline and naphthoquinone moieties respectively, on the catalytic site. This could be possible due to π-π interactions, established between Y343 and the aromatic systems. Meanwhile, the other aromatic extreme of both molecules (naphthalene and biphenyl, respectively) interacts with W333, via π-π, as well as the formation of a hydrogen bond with H235 (Figures 1G and 2B,C). As far as we know,

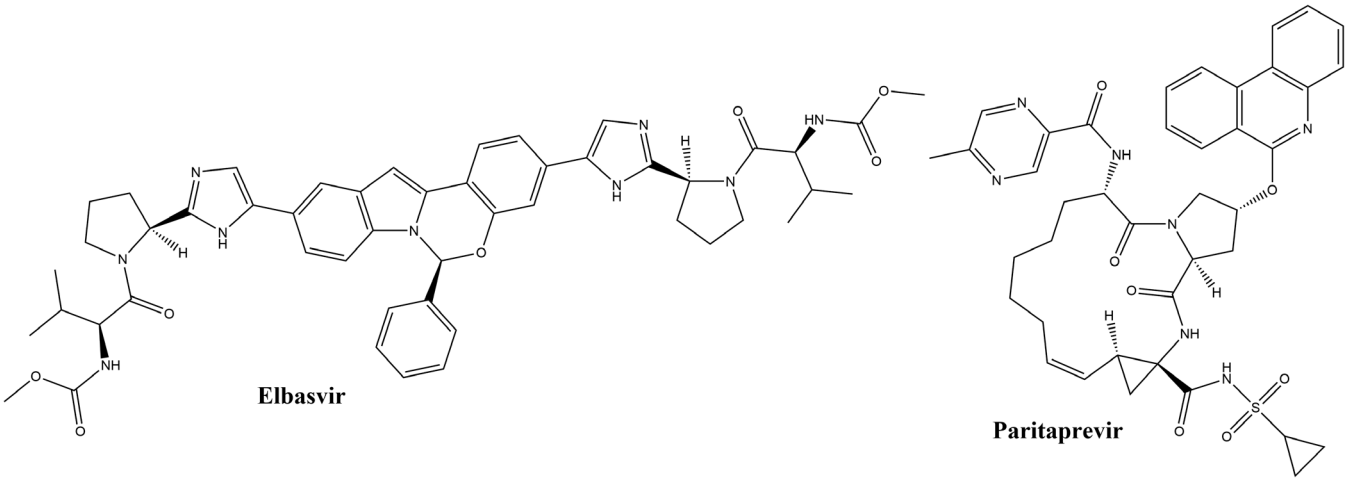

SCHEME 1 Elbasvir and Paritaprevir, drugs proposed with possible activity against Nsp15 of SARS-CoV-2, obtained by virtual screening approach

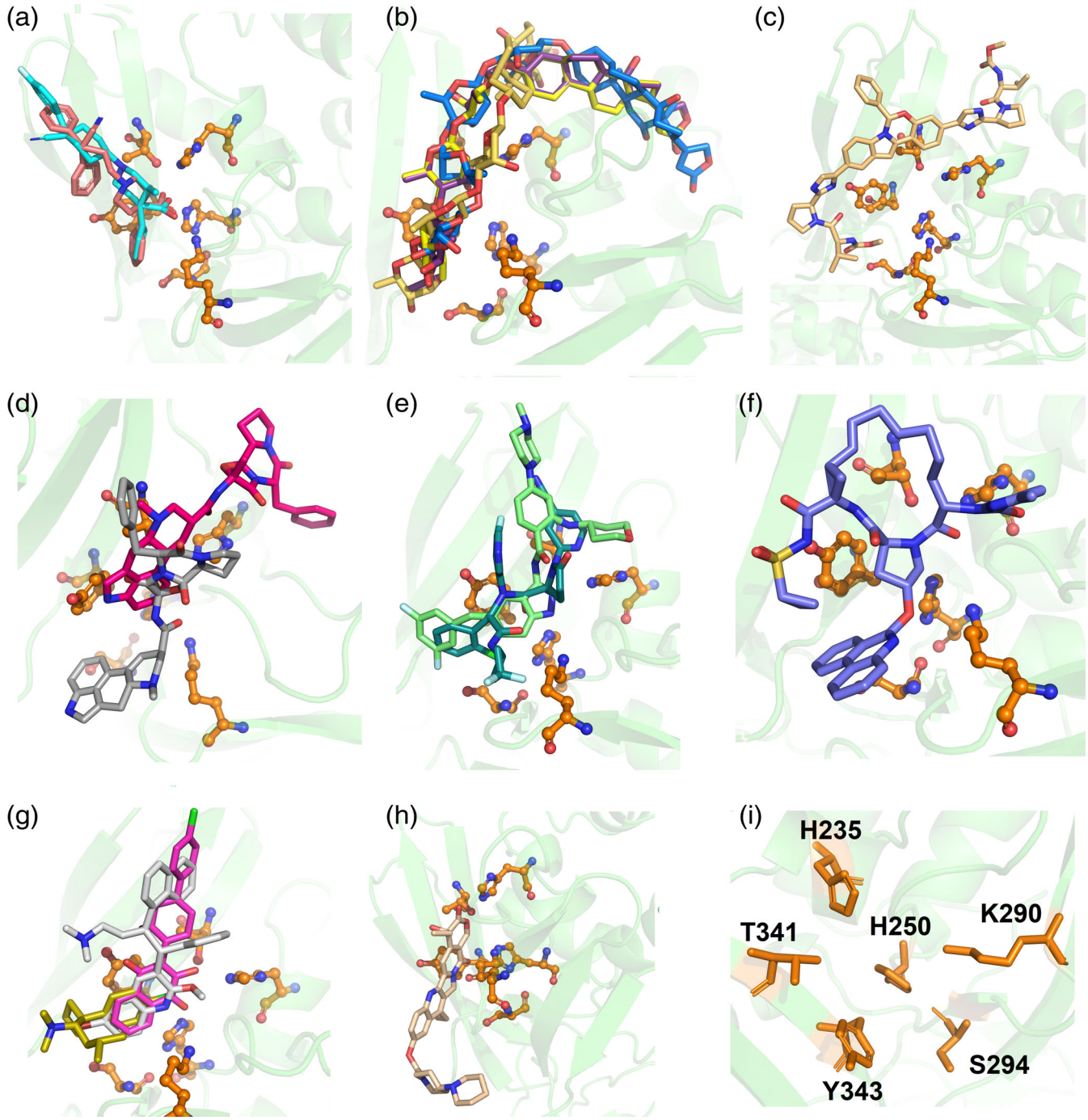

FIGURE 1 Binding poses of the 16 compounds selected by virtual screening obtained by molecular docking simulations against Nsp15 of SARS-CoV-2. (A) Difenoxine and Levocabastine (shown in color light pink and cyan, respectively), (B) Digoxin, Deslanoside, Acetyldigitoxin, Digitoxin (shown in color yellow-orange, marine, violet purple and yellow, respectively), (C) Elbasvir (shown in color wheat), (D) Ergotamine and dyhydroergotamine (shown in magenta and gray, respectively), (E) Ivosidenib and entrectinib (shown in color deepteal and tvgreen, respectively), (F) Paritaprevir (slate color), (G) Atavaquone, Bedaquiline, Sibutramine (shown in magenta, gray and olive color, respectively), (H) irinotecan (shown in wheat color), (I) Nsp15 and close up of the catalytic site. Nsp15 are depicted as green cartoon and residues belonging to catalytic site as orange ball and stick, ligands are depicted as stick

this is the first time that Bedaquiline has been suggested for its use in the Nsp15 inhibition. In the case of Atovaquone, it has been suggested as a Mpro ligand with antiviral efficacy,[24] which also could be due to Nsp15 inhibition.

Sibutramine accommodates its phenyl ring into the catalytic site, similarly to Atovaquone and Bedaquiline. Its anchorage is mainly due to π-π interaction with Y343, and is supported by hydrophobic interactions with the following residues: H25 and V292, K290, C291,

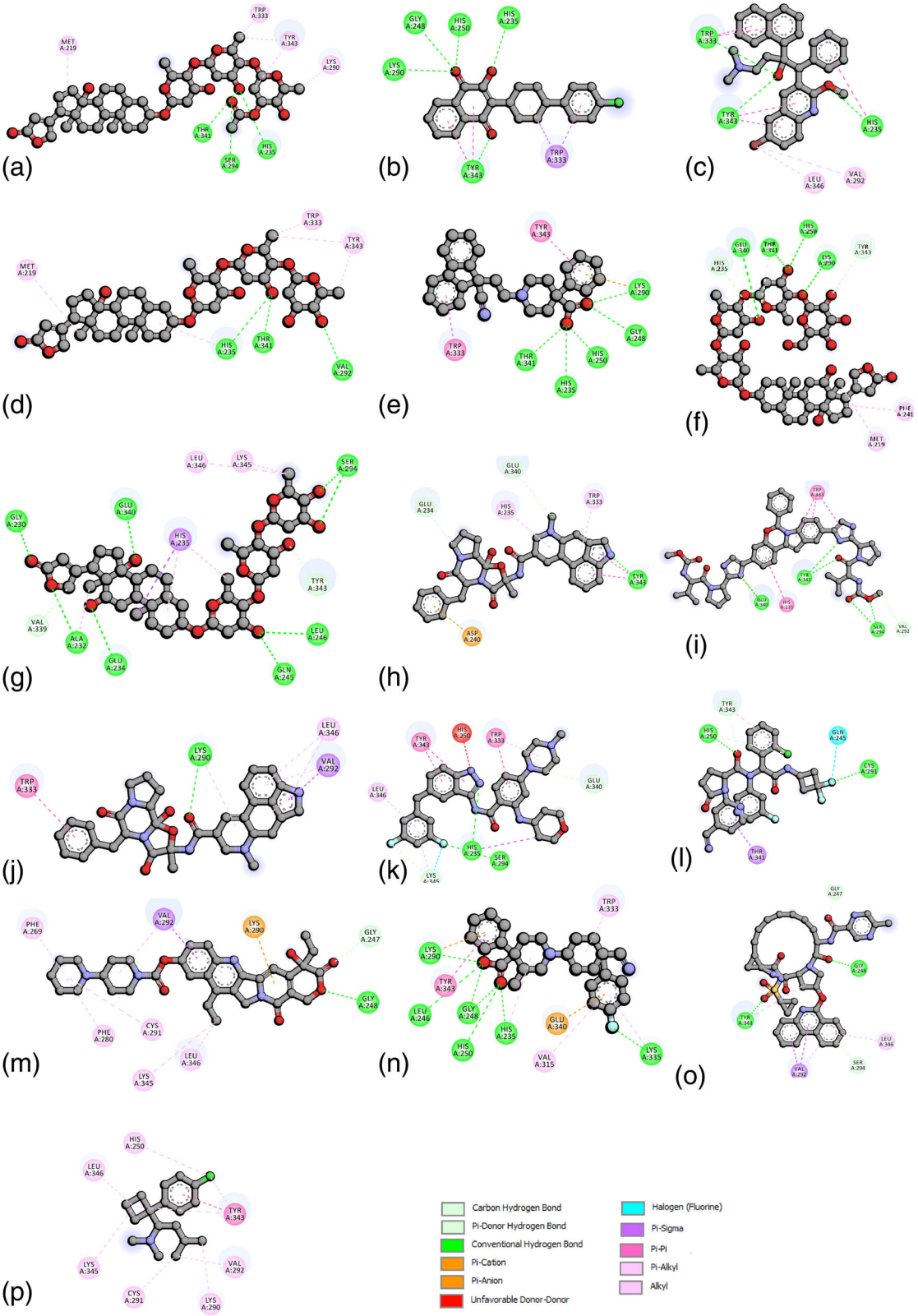

FIGURE 2 Interactions observed between ligands and NSP15 of SARS-CoV-2 obtained by molecular docking. (A) Acetyldigitoxin, (B) Atavaquone, (C) Bedaquiline, (D) Digitoxin, (E) Difenoxin, (F) Deslanosido, (G) Digoxin, (H) Dihydroergotamine, (I) Elbasvir, (J) Ergotamine, (K) Entrectinib, (L) Ivodesinib, (M) Irinotecan, (N) Levocabastin, (O) Paritaprevir, (P) Sibutramine. Interactions are color coded as indicated at the right bottom of the figure, that was built using discovery studio V16[26]

K345, and L346. Sibutramine could have not been taken as starting point for Nsp15 drug repurposing due to it was withdrawn due to safety concerns, particularly it increases stroke and myocardial infarction risk.[29,30]

Even though Ergotamine and Dihydroergotamine are chemically similar compounds, they show very different binding modes, fact that can be reflected on their binding free energies (Table 1, Figure 1D). Dihydroergotamine showed better binding free energy than Ergotamine. The former ligand accommodates the ergoline ring in the catalytic site, interacting with Y343 via π-π, and with H235 and W333, via π-alkyl, as well as with residues surrounding the catalytic site via hydrophobic interactions (E234 and E340, D240) (Figure 2H). On the other hand, Ergotamine protruded the ergoline ring to the opposite direction, while interacting with residues such as L346 and V292. Its phenyl ring interacts with W333, and forms a hydrogen bond with the oxygen of the amide portion (Figure 2J). This binding mode is energetically less favorable and this coincides with the decreased free binding energy value. The same tendency in binding affinity was predicted by another in silico study.[31]

Paritaprevir reaches the catalytic site and accommodates its macrocyclic portion and protruded toward the exterior, with the substituents that stabilize the structure (Figure 1F). Hydrogen bonds are formed between Y343, and oxygen of the sulphonamide, with the residue: G247 and G248 with the oxygen of the amide portion and oxygen of the macrocyclic hydroxyl group; as well as hydrophobic interactions with phenanthridine portion (V29, S294, and L346) (Figure 2O).

Elbasvir is accommodated along with the catalytic site, mainly by π-π interactions with W333 and H235. Hydrogen bonds are also observed with the residues Y343, S294, and E340 (Figures 1C and 2I).

Irinotecan inserts its Pyranoindolizinoquinolines moiety into the catalytic site where a hydrogen bond is formed with G248, and a π-cation interaction with K290. The Binding mode of this ligand is mainly governed by hydrophobic interactions (G247, V292, K345, L396, F280, C291, and F269) (Figure 2H,M).

Molecular docking of these compounds, showed that molecules with good binding energy values against Nsp15, are those that are capable of establishing π-π interactions, as well as hydrogen bonds, and other non-bonded interactions, albeit to a less grade.

3.3 | MD simulations

3.3.1 | Structural analysis

Thirty Nano seconds MD simulations of the Apo-Nsp15 system, as well as the complexes: Nsp15-Elbasvir, Nsp15-Paritaprevir, and Nsp15-Citrate were performed (Figure 3). From these RMSD results, it could be observed that the compounds: Elbasvir (RMSD: 1.8856 ± 0.2136) and Paritaprevir (RMSD: 2.20482 ± 0.4325) provide higher stability to the Nsp15 structure (RMSD: 4.86436 ± 0.7354), in a similar way that Citrate does to Nsp15 crystal structure (RMSD: 2.1316 ± 0.2936) (PDB: 6 W01).[6,31]

RMSF results indicate that, in general, the highest peaks are observed in the following residue segments: (I27-E42, V166-T175, and G337-347Q). Interestingly, the probed compounds promoted stabilization to the protein structure, particularly in the H250-E340 residue segment. This information coincides well with the docking analysis, which suggest that for all cases, residues of the Nsp15 protein, within the H250-R340 residue segment, interact with the mentioned compounds, by showing mainly aromatic and π-π interactions in most of the cases.

3.3.2 | Clustering analysis

The Clustering analysis allow us to obtain the most representative ensembles from the equilibrium phase of the MD simulation, by considering the last 30 ns. The most populated conformations were concentrated in the first three clusters, from which more than 99% are represented for apoprotein, and in complex with Elbasvir and Patiraprevir, whereas 96% was represented by Citrate (Table 2).

The most populated cluster conformation of the Apo Nsp15, depicts several differences regarding the native conformation as the RMSD and RMSF analysis suggests. Additionally, the native conformation of Nsp15 was structurally compared against the conformation retrieved from the most populated cluster conformation and an RMSD of 5.04 Å. Major differences were observed at NendoU catalytic domain, in the N-terminal oligomerization domain, and at protein extremes, while the middle domain remains with fewer changes

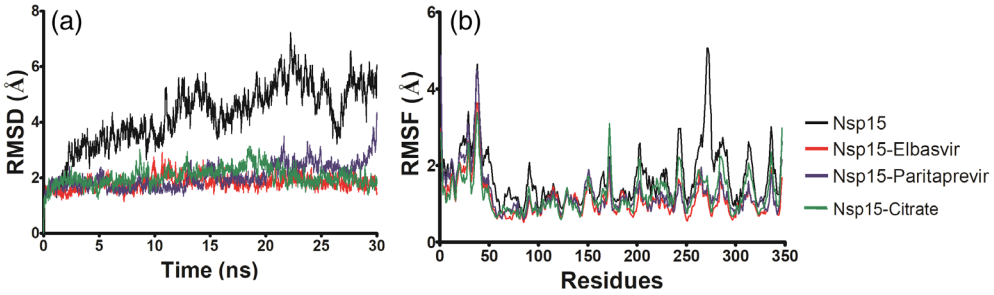

FIGURE 3 Geometrical parameters of 30 ns MD simulations. Carbon alpha atoms were considered for the calculations employing GROMACS program. (A) RMSD and (B) RMSF. Apo Nsp15 is depicted as black lines, while complex Nsp15-Elbasvir is depicted in red and Nsp15-Paritaprevir is depicted as blue line

TABLE 2 Cluster analysis using RMSD cut-off of 2.0 A

	Cluster population (%)								
System	**1**	**2**	**3**	**4**	**5**	**6**	**7**	**8**	**9**
Nsp15	91.95	4.94	3.05	0.05					
Nsp15-Elbasvir	78.81	12.60	4.65	2.95	0.49	0.19	0.15	0.09	0.04
Nsp15-Paritaprevir	84.80	7.74	6.54	0.54	0.25	0.05	0.05		
Nsp15-Citrate	93.50	4.24	1.69	0.39	0.15				

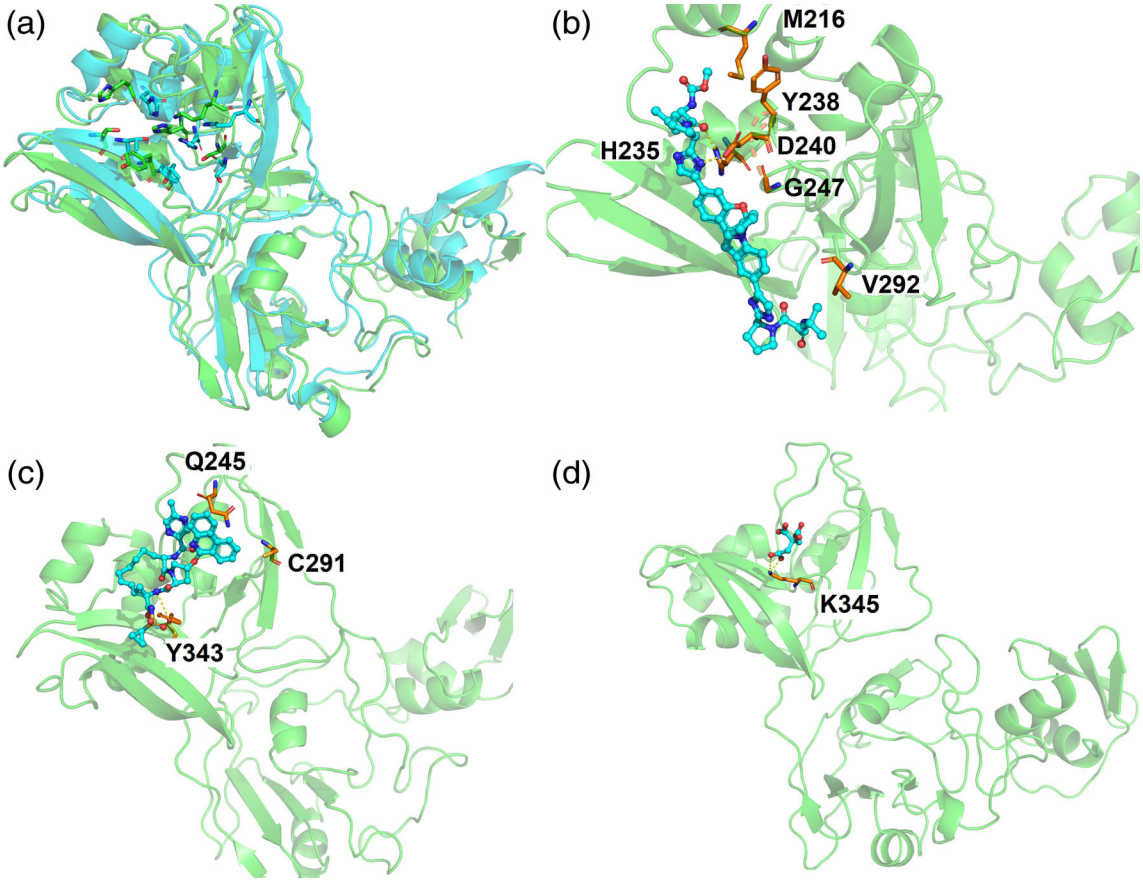

FIGURE 4 Most populated cluster conformation retrieved from the MD simulation. (A) Apo Nsp15, (B) Nsp15-Elbasvir, (C) Nsp15-Paritaprevir and (D) Nsp15-citrate. In panel A native Nsp15 is overlapped with most populated cluster conformation of apo Nsp15. Native Nsp15 is depicted as cyan ribbon, while most populated cluster conformation of each system is depicted as green ribbon. Ligands are depicted as cyan ball and stick and the residues with which ligands interacted are depicted as orange sticks

(Figure 4A). The Holo systems showed fewer changes in the ligand-protein complex. The comparison of Nsp15-Elbasvir complex native structure against the most populated cluster conformation shows a RMSD of 1.124 Å, and depicts particular changes at the following segments: M220-G247 and D301-L332, which are part of the NendoU domain, mainly formed by residues that do not interact with Elbasvir (Figure 4B). Nsp15-Paritaprevir complex shows a RMSD of 1.501 Å, and depicting some differences at the following segments: S2-E42, G170-V173, R225-E229, S262-S274, K308-V319, which are located at both the N-terminal oligomerization domain and the NendoU catalytic domain (Figure 4C). While, the comparison of the native structure versus the most populated cluster conformation of Nsp15-citrate shows a RMSD of 1.246 Å, with structural differences at the following segments: S2-I31, V36-T48, G170-K174, S198- E203, Y238-F269, localized along with the protein structure (Figure 4D). As can be seen, the ligands stabilize the Nsp15 protein structure and the tendency is in agreement with geometrical parameters (RMSF and RMSD).

In the detailed analysis of the interactions, we found that in the most populated cluster conformations of the complex Nsp15-Elbasvir, Elbasvir forms a double hydrogen bond with H235, as well as hydrophobic interactions with the following residues: M216, Y238, D240, G247, and V292. It was also observed that it remains within the catalytic site, forming a stable complex (Figure 4B). In the case of Paritaprevir, it forms a hydrogen bond with Y343, as well as

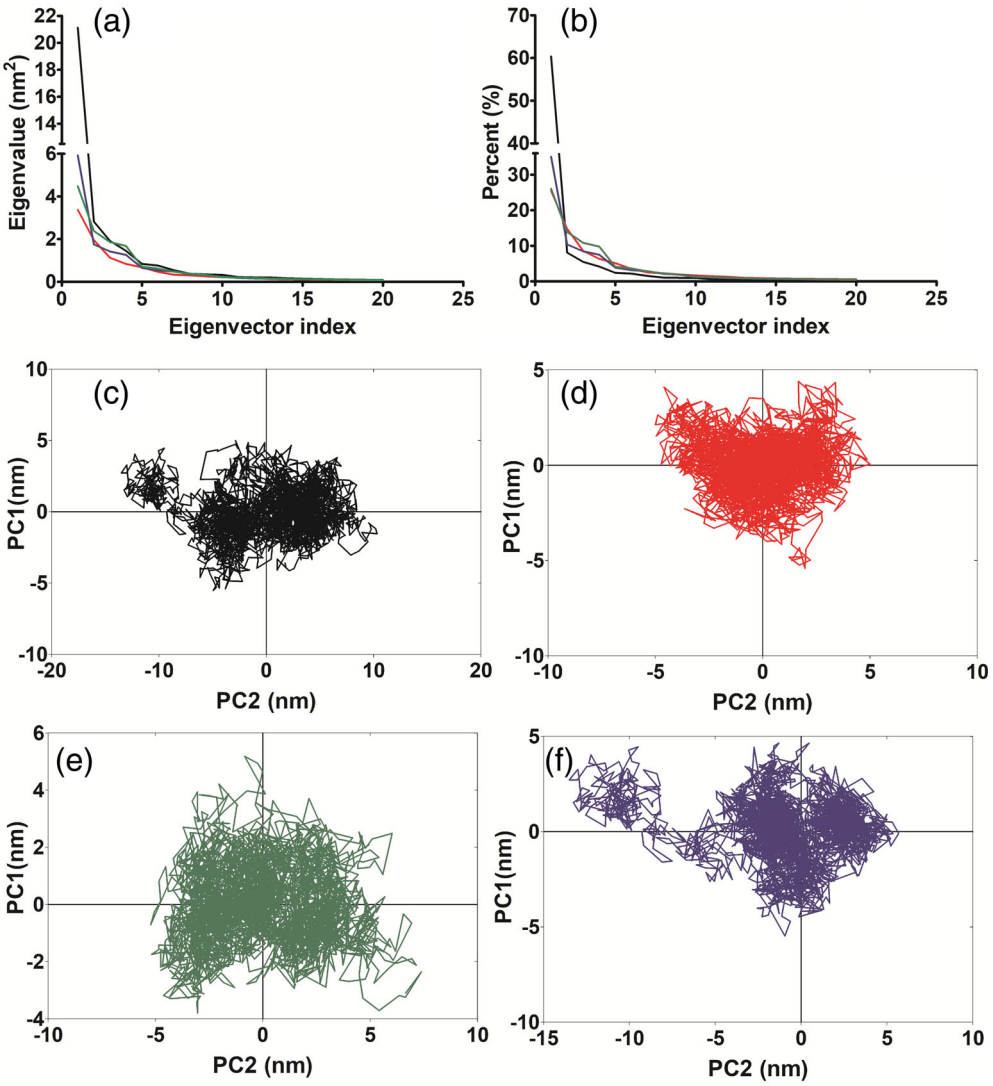

FIGURE 5 Principal component analysis of apo-Nsp15 and holo trajectories. (A) The first 20 eigenvectors of the covariance matrix, (B) Percentage of each eigenvectors vs eigenvalues, only the first 20 eigenvectors are depicted, (C) projection of the motion in the phase space along the first and second eigenvectors (PC2 vs. PC1) of the apo Nsp15, (D) projection of the motion in the phase space along the first and second eigenvectors (PC2 vs. PC1) of the complex Nsp15-Elbasvir, (E) projection of the motion in the phase space along the first and second eigenvectors (PC2 vs. PC1) of the complex Nsp15-Paritaprevir, (F) projection of the motion in the phase space along the first and second eigenvectors (PC2 vs. PC1) of the complex Nsp15-citrate. Nsp15 are depicted in black, Nsp15-Elbasvir in red, Nsp15-Paritaprevir in green and Nsp15-citrate in purple

hydrophobic interactions with Q45 and C291 (Figure 4C). Finally, Citrate only binds to K345 (Figure 4C). Our results are consistent with other studies, where was citrate was reported as Nsp-15 structure stabilizer.[31]

3.3.3 | Principal component analysis

In order to elucidate the principal components that contribute to the global fluctuations of apo and holo Nsp15 systems, the PCA analysis of the MD trajectories was performed (Figure 5A). According to PCA analysis, the total motions were dispersed along 3000 eigenvectors, where the first 20 eigenvectors contributed to the collective motions (91.5%, 80.9%, 84.0%, and 83.8% for apo Nsp15, Nsp-Elbasvir, Paritaprevir, and citrate) (Figure 5B).

While inspecting the projections for the first and second eigenvectors (PC1 vs. PC2) of the systems, we were able to capture 40% to 68% of the collective motions (Figure 5C-F), which can be seen by projections onto the essential subspace, that were basically differences between the mobility in the apo and holo systems. The apo Nsp15 exhibited the highest fluctuation along the first and second eigenvectors in comparison with holo systems, supporting the higher fluctuations observed in the apoprotein (Figure 5C), followed by Nsp15-citrate complex, which resembles the mobility behavior of apo Nsp15 (Figure 5F), but with reduced conformed distribution along the subspace. This behavior is corroborated by comparing Figure 6A, D, where apo Nsp15 and Nsp15-Citrate complex, respectively, illustrated that Citrate also presented movement in the middle region as the apoprotein does, while Nsp15-Elbasvir (Figure 6B) and Nsp15-Paritaprevir (Figure 6C) complexes did not show this structural behavior. Therefore, it supports the fact that citrate does have an impact on the conformational mobility, as RMSF, RMSD, and clustering analysis suggest, although maintaining the movement in some regions, like the apoprotein. On the other hand, Nsp15-Elbasvir and Nsp15-Paritaprevir complexes (Figure 5D,E, respectively) show a more compact trajectory over the cluster distribution phase space, indicating that protein motions were reduced by the binding of both compounds. Nsp15-Elbasvir complex was one of the most defined

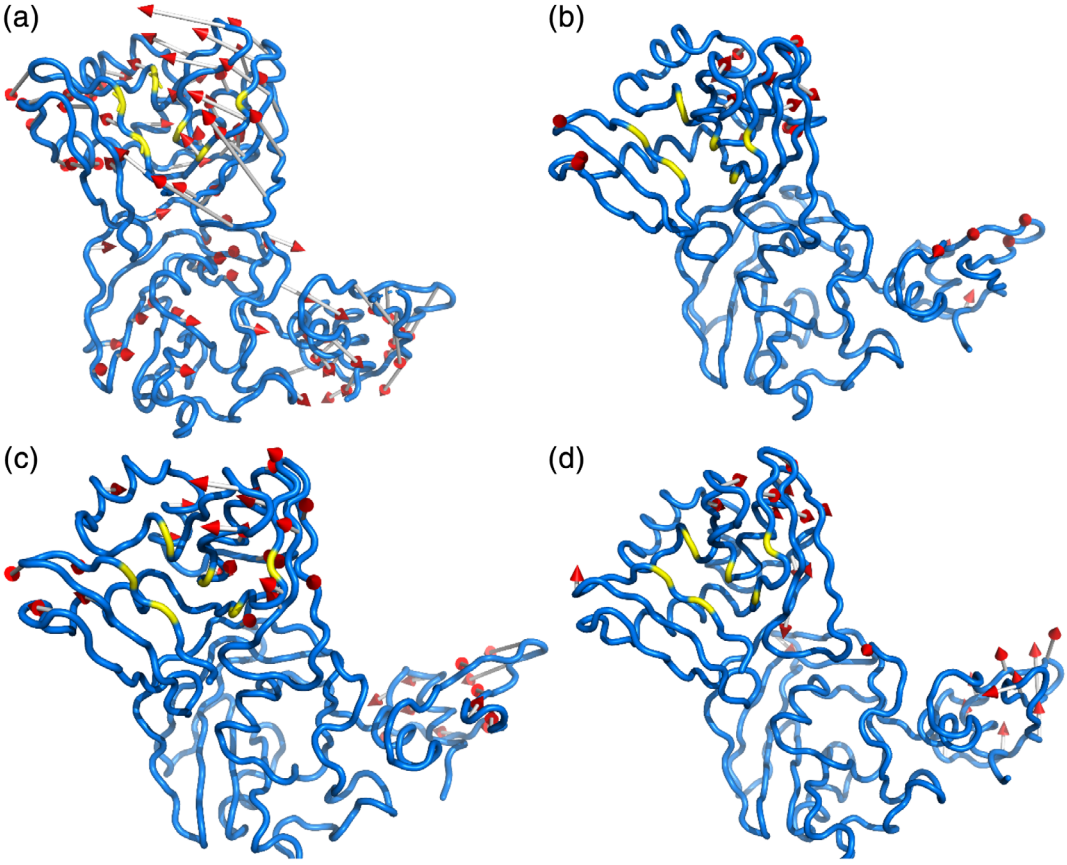

FIGURE 6 Graphical representation of the two extreme projections. Representation of the two extreme projections along the first eigen vector of MD simulation of (A) apo Nsp15, (B) Nsp-Elbasvir, (C) Nsp15-Paritaprevir, and (D) Nsp15-citrate

and stable cluster distribution along the subspace (Figure 5D, in comparison to both Paritaprevir and citrate. Thus, these results suggest that Elbasvir and, to a lesser degree Paritaprevir, are better compounds to promote protein stabilization, compared with citrate.These findings are graphically corroborated with the porcupine representation, which allowed us to characterize the collective motion along PC1 and PC2, by providing better visualization of the direction and magnitude of the motions that mainly contribute to the entire mobility. A similar mobility decrease was reported due to the ligand-binding process, and with possible activity as inhibitor, as reported in another previous work.[31] The motions on apo Nsp15 are distributed along with the whole structure (Figure 6A), whereas the ligands showed a motion decrement, compared in comparison to apoprotein. In the case of the Nsp15-Citrate complex (Figure 6D), in general, it showed a lower conformational mobility compared with the apoprotein. Particularly, the Nsp15-Citrate complex showed a higher mobility at the NendoU (D336, Y238-N245, T282-S289, R258-L266, and S198-F204) and N-terminal oligomerization regions (E171-V173), with a lower mobility in the middle region (N46-K47, Y33-L43, I28-N30, and S2-N25). This indicates it has a similar behavior than apo Nsp15. Regarding Elbasvir and Paritaprevir, their mobility was decreased, compared with the apo Nsp15 and Nsp15-Citrate systems. Interestingly, both complexes concentrated their motions at NendoU region (its catalytic portion), as well as in the N-terminal oligomerization regions, with almost null changes in the middle region (Figure 6). Specifically, Elbasvir presented higher motions mainly in the NendoU regions: C334-G337, L312-K317, S242-L246, T282-S289, R258-L266, and L201-L217) and K35-T49, V11-N12, all of which belong to N-terminal oligomerization regions (Figure 6B). Similarly, Paritaprevir had a higher mobility, although with a wider spanning region than Elbasvir, which involves the following segments: D311-S316, W333-E340, L252-F269, M272-S274, Y279-C293, N197-G230, and F241-G247, all of which are NendoU regions, and M1-E31 and E42-T34, which are N-terminal oligomerization regions (Figure 6C). All these findings are in agreement with RMSF and clustering analysis, highlighting the impact to the Nsp15 mobility, due to the ligand-binding process.

4 | CONCLUSIONS

SARS-CoV and SARS-Cov-2 are members of *Cornaviridae* subfamily and the both viruses are able to infect human. Particularly, SARS-CoV-2 is responsible for the outbreak of COVID'19 which began in China in 2019.

These coronaviruses are formed by structural and non-structural proteins. In general, most of the research has been focused on the former ones. However, the study of the non-structural proteins is of

worthy interest, since Nsp15 proteins from both groups, have very similar catalytic sites, and share a high identity and similarity. Thus, the aim of this work was to search for potential drugs available in the DrugBank database, that would target the SARS-CoV-2 Nsp15 protein, as an alternative treatment for the COVID-19 disease. This procedure was done by means of different computational approaches, such as docking studies, molecular dynamics simulations, clustering, and Principal Component analysis.

From our docking analysis, we were able to observe that the antiviral drugs: Paritaprevir and Elbasvir, had the lowest free binding energy values, from an initial list of 15 compounds. Interestingly, while observing the molecular interactions from the cluster conformations analysis, we could observe that both compounds, form hydrogen bonds as well hydrophobic interactions, which leads to stable Nsp-15 complexes. Additionally, a similar structural stability was reached for the Nsp-15-Citrate complex. As part of the structural studies, Molecular dynamics simulations studies of the Apo and Holo- Nsp15 systems bring interesting insights about the stability of these protein-ligand complexes, and observe structural differences Finally, from the PCA analysis, we depicted that Nsp15-Elbasvir and Paritaprevir complexes, showed a more compact cluster distribution. This observation indicates that motions were reduced due to the binding of those compounds on the Nsp15 structure. Thus, suggesting that Elbasvir and Paritaprevir (to a lower degree), successfully promoted protein structure stabilization, compared with Nsp15-Citrate complex.

ACKNOWLEDGMENTS

We gratefully acknowledge to CONACYT, to Instituto Politécnico Nacional, to COFAA-SIP/IPN and YSL thanks to CONACYT by PhD scholarship.

ORCID

Yudibeth Sixto-López https://orcid.org/0000-0001-8903-3834
Marlet Martínez-Archundia https://orcid.org/0000-0002-6140-8953

REFERENCES

[1] A. R. Fehr, S. Perlman, in *Methods in Molecular Biology* (Ed: N. J. Clifton) Humana Press, New York, NY **2015**, p. 1.
[2] P. A. Rota, M. S. Oberste, S. S. Monroe, W. A. Nix, R. Campagnoli, J. P. Icenogle, S. Penaranda, B. Bankamp, K. Maher, M. H. Chen, S. Tong, A. Tamin, L. Lowe, M. Frace, J. L. DeRisi, Q. Chen, D. Wang, D. D. Erdman, T. C. Peret, C. Burns, T. G. Ksiazek, P. E. Rollin, A. Sanchez, S. Liffick, B. Holloway, J. Limor, K. McCaustland, M. Olsen-Rasmussen, R. Fouchier, S. Gunther, A. D. Osterhaus, C. Drosten, M. A. Pallansch, L. J. Anderson, W. J. Bellini, *Science* **2003**, *300*, 1394.
[3] N. Zhu, D. Zhang, W. Wang, X. Li, B. Yang, J. Song, X. Zhao, B. Huang, W. Shi, R. Lu, P. Niu, F. Zhan, X. Ma, D. Wang, W. Xu, G. Wu, G. F. Gao, W. Tan, *N Engl J Med* **2020**, *382*, 727.
[4] A. A. T. Naqvi, K. Fatima, T. Mohammad, U. Fatima, I. K. Singh, A. Singh, S. M. Atif, G. Hariprasad, G. M. Hasan, M. I. Hassan, *Biochim Biophys Acta Mol basis Dis* **2020**, *1866*, 165878.
[5] A. C. Walls, Y. J. Park, M. A. Tortorici, A. Wall, A. T. McGuire, D. Veesler, *Cell* **2020**, *181*, 281 e286.
[6] Y. Kim, R. Jedrzejczak, N. I. Maltseva, M. Wilamowski, M. Endres, A. Godzik, K. Michalska, A. Joachimiak, *Protein Sci* **2020**, *29*, 1596.
[7] Kao, *Virus Adaptation and Treatment* **2010**, *2010*, 125.
[8] S. Xia, M. Liu, C. Wang, W. Xu, Q. Lan, S. Feng, F. Qi, L. Bao, L. Du, S. Liu, C. Qin, F. Sun, Z. Shi, Y. Zhu, S. Jiang, L. Lu, *Cell Res* **2020**, *30*, 343.
[9] K. Bhardwaj, S. Palaninathan, J. M. Alcantara, L. L. Yi, L. Guarino, J. C. Sacchettini, C. C. Kao, *J Biol Chem* **2008**, *283*, 3655.
[10] J. S. M. Peiris, *Medical Microbiology*. Churchill Livingstone, UK **2012**, p. 587.
[11] X. Deng, S. C. Baker, *Virology* **2018**, *517*, 157.
[12] Senanayake, S. L. Future Drug Discovery **2020**.
[13] A. Nitsche, B. Schweiger, H. Ellerbrok, M. Niedrig, G. Pauli, *Emerg Infect Dis* **2004**, *10*, 1300.
[14] K. A. Ivanov, T. Hertzig, M. Rozanov, S. Bayer, V. Thiel, A. E. Gorbalenya, J. Ziebuhr, *Proc Natl Acad Sci U S A* **2004**, *101*, 12694.
[15] S. Forli, R. Huey, M. E. Pique, M. F. Sanner, D. S. Goodsell, A. J. Olson, *Nat Protoc* **2016**, *11*, 905.
[16] O. Trott, A. J. Olson, *J Comput Chem* **2010**, *31*, 455.
[17] G. M. Morris, R. Huey, W. Lindstrom, M. F. Sanner, R. K. Belew, D. S. Goodsell, A. J. Olson, *J Comput Chem* **2009**, *30*, 2785.
[18] W. R. P. Scott, P. H. Hünenberger, I. G. Tironi, A. E. Mark, S. R. Billeter, J. Fennen, A. E. Torda, T. Huber, P. Krüger, W. F. van Gunsteren, *Chem A Eur J* **1999**, *103*, 3596.
[19] B. Hess, H. Bekker, H. J. C. Berendsen, J. G. E. M. Fraaije, *J Comput Chem* **1997**, *18*, 1463.
[20] E. Lindahl, B. Hess, D. van der Spoel, *J Mol Model* **2001**, *7*, 306.
[21] A. Amadei, A. B. Linssen, H. J. Berendsen, *Proteins* **1993**, *17*, 412.
[22] Y. Sixto-Lopez, M. Bello, R. A. Rodriguez-Fonseca, M. C. Rosales-Hernandez, M. Martinez-Archundia, J. A. Gomez-Vidal, J. Correa-Basurto, *J Biomol Struct Dyn* **2017**, *35*, 2794.
[23] S. Matsuyama, M. Kawase, N. Nao, K. Shirato, M. Ujike, W. Kamitani, M. Shimojima, S. Fukushi, *J. Virol* **2020**, *95*.
[24] Ayman, F.; Ping, W.; Ian N.B.; Jennifer, L. E.; Maikke B. O.; Wenchun, F.; Matthew B. M.; Mahmoud, A.; John, W. S.; Hesham, S. Identification of Atovaquone, Ouabain and Mebendazole as FDA Approved Drugs Tar-geting SARS-CoV-2 (Version 4), **2020**.
[25] Sangjae, S.; Jung Woo, P.; Dosik, A.; Junwon, Y.; Hyojung, P.; Soonwook, H. Supercomputer-aided Drug Repositioning at Scale: Virtual Screening for SARS-CoV-2 Protease Inhibitor, **2020**.
[26] Discovery Studio, *Dassault Systèmes*, BIOVIA, Dassault Systèmes, San Diego **2016**.
[27] Ko, M.; Chang, S. Y.; Byun, S. Y.; Choi, I.; d'Alexandry d'Orengiani, A.-L. P. H.; Shum, D.; Min, J.-Y.; Windisch, M.P. **2020**, The COVID-19 Gene and Drug Set Library.
[28] S. Jeon, M. Ko, J. Lee, I. Choi, S. Y. Byun, S. Park, D. Shum, S. Kim, *Antimicrob Agents Chemother* **2020**, *64*, 7.
[29] S. Czernichow, G. D. Batty, *Obes Facts* **2010**, *3*, 155.
[30] FDA, FDA Drug Safety Communication: FDA Recommends Against the Continued Use of Meridia (sibutramine), https://www.fda.gov/drugs/drug-safety-and-availability/fda-drug-safety-communication-fda-recommends-against-continued-use-meridia-sibutramine (Accesed: January 28, 2021).
[31] A. Chandra, V. Gurjar, I. Qamar, N. Singh, *J Biomol Struct Dyn, Epub* **2020**, 1.

How to cite this article: Sixto-López Y, Martínez-Archundia M. Drug repositioning to target NSP15 protein on SARS-CoV-2 as possible COVID-19 treatment. *J Comput Chem*. 2021;42:897–907. https://doi.org/10.1002/jcc.26512